

ISES SWC2015

Analysis of Fluid Flow and Heat Transfer inside a Spherical Container Encapsulated by Molten Salt

Adrián Belinchón Ovejero, Selvan Bellan, José González-Aguilar, and Manuel Romero

IMDEA Energy Institute, Ramon de la Sagra 3, 28935 Móstoles, Spain

Abstract

A mathematical model of melting process inside a spherical container, which is filled with phase change material, is developed to describe the characteristics of heat transfer and flow inside the capsule for high temperature storage systems. The finite element method is used to solve continuity, momentum and energy equations. The main intention of this investigation is to derive a dimensionless correlation for effective thermal conductivity. The correlation can be used in packed bed models to study the thermal performance of the thermal energy storage systems. The capsule is filled with sodium nitrate since its melting point is in the operation range of concentrated solar power plant. The shell of the capsule is made up of nickel, which is uniformly heated at the external surface. The enthalpy-porosity method is used to track the solid-liquid interface. The model is, validated with the reported experimental results, used to investigate the influence of pellet size and Stefan number.

Keywords: Thermal energy storage system; Latent heat; Melting of PCM; Effective thermal conductivity

1. Introduction

In latent heat thermal energy storage systems packed with spherical pellets, the phase change process inside the pellets plays a vital role since the overall performance of the storage tank depends on this process. Thus, it has been received great importance, considerable number of investigations on this subject has been made by both theoretically and experimentally (Assis et al., 2007; Felix et al., 2006; Hosseinizadeh et al., 2012; Ismail and Henríquez, 2000). One dimensional conduction models were developed, to study the phase change process inside a spherical capsule, by assuming the solid portion of the PCM remains at the center of the sphere, neglecting the solid core movements (e.g. Felix et al., 2006; Ismail and Henríquez, 2000). Two dimensional axisymmetric models were developed to study the flow, natural convection-dominated melting, and the movement of the solid PCM portion during melting process (e.g. Assis et al., 2007; Hosseinizadeh et al., 2012). The melting of n-octadecane in a glass spherical container was investigated numerically and experimentally by Moore and Bayazitoglu (1982) and found that the natural convection effects can be neglected at small Stefan numbers. Bareiss and Beer (1984) investigated the phase change process in cylindrical geometries; the predicted melting rate showed good agreement with the experimental data presented by Moore and Bayazitoglu (1982). Using the analysis made by Bareiss and Beer (1984), an analytical solution for the melting rate at the lower surface of the solid core in a spherical capsule was presented by Roy and Sengupta (1987).

The melting process of n-octadecane in an open spherical glass container was numerically investigated by Hosseinizadeh et al. (2012). A uniform temperature boundary condition was imposed at the outer wall of the shell. The developed model was validated with the experimental results reported by Tan (2008). Furthermore, a number of experimental and analytical investigations have been made on the heat transfer and buoyancy driven flow during melting of PCM inside spherical capsules. However, the literature survey shows that most of the past studies focused on low temperature storage applications. The literature is lack of

melting of PCM in the closed container in high temperature range, especially in the operation range of parabolic CSP plants (300-500 °C). Accordingly, this study aims at developing a two dimensional axisymmetric model to study the natural convection dominated melting process inside a spherical container in high temperature range and, to derive the dimensionless correlation of effective thermal conductivity for packed bed models.

2. Mathematical modeling

The computational domain is shown in Fig.1. An axi-symmetric model is developed by assuming the solid and liquid phases of the PCM are homogeneous and isotropic; the flow is laminar and incompressible; the phase change process takes place in the interval between 306.3°C and 306.8°C; where the density in the mushy zone varies linearly from 2130 kg/m³ to 1908 kg/m³. The temperature dependent liquid phase density is defined as (Archibold et al., 2014)

$$\rho_{liq} = \rho_m / \beta(T - T_m) + 1 \quad (\text{eq. 1})$$

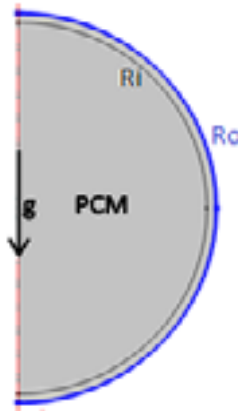


Fig.1: The computational domain

As the PCM volume changes during the phase change process, the elastic deformation takes place in the shell material (Archibold et al., 2014; Tanvir et al., 2015). The enthalpy-porosity method is used in the phase change range, by which the porosity in each element is equal to the liquid fraction in that element. Thus, the porosity is zero in solid regions. Based on the foregoing assumptions, the governing equations; continuity, momentum, and energy, are;

$$\frac{\partial \rho}{\partial t} + \nabla \cdot (\rho \vec{V}) = 0 \quad (\text{eq. 2})$$

$$\rho \frac{\partial \vec{V}}{\partial t} + \rho (\vec{V} \cdot \nabla) \vec{V} = -\nabla P + \nabla \cdot [\mu (\nabla \vec{V} + (\nabla \vec{V})^T)] + \rho \vec{g} + A(\gamma) \vec{V} \quad (\text{eq. 3})$$

$$\rho \frac{\partial h}{\partial t} + \rho \vec{V} \cdot \nabla h = \nabla \cdot (k \nabla T) \quad (\text{eq. 4})$$

where ρ , \vec{V} , P , μ , k , h and T are density, velocity vector, pressure, dynamic viscosity, thermal conductivity, specific enthalpy and temperature respectively. The porosity function $A(\gamma)$ is defined by Eq. (5)

$$A(\gamma) = \frac{C(1-\gamma)^2}{\gamma^3 + \epsilon} \quad (\text{eq. 5})$$

where the computational constant (ϵ), and the melting front morphology constant (C) are 0.001 and 10⁵ kg/m³s respectively. The specific enthalpy (h) is defined as the sum of the sensible enthalpy h_{sen} and enthalpy change due to phase change γL , where L is the latent heat of the material. The melt fraction, γ , is defined by eq. (6). Thermo-physical properties of the sodium nitrate are given in Table 1. The finite element method based commercial software COMSOL multiphysics 4.2 (2014) is used to solve the governing equations. In

order to optimize the mesh of the model, grid dependent tests were carried out for four various mesh distributions; the total number of elements was 5012, 10046, 14066 and 18506 respectively. The results given by the mesh generated with 10046 elements were, significantly deviated from the mesh with 5012 elements, analogous to the results produced by 14066 and 18506 elements. Thus, the mesh with 10046 elements was used for all calculations.

$$\gamma = \begin{cases} 0 & \text{if } T < T_{sol} \\ \frac{T - T_{sol}}{T_{liq} - T_{sol}} & \text{if } T_{sol} \leq T \leq T_{liq} \\ 1 & \text{if } T > T_{liq} \end{cases} \quad (\text{eq. 6})$$

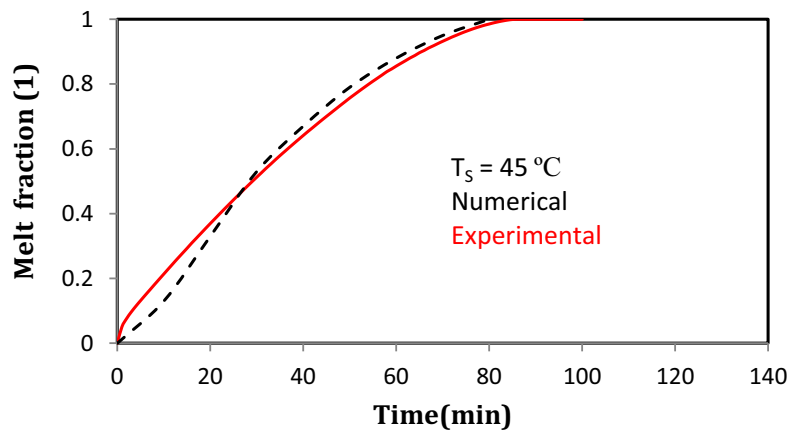
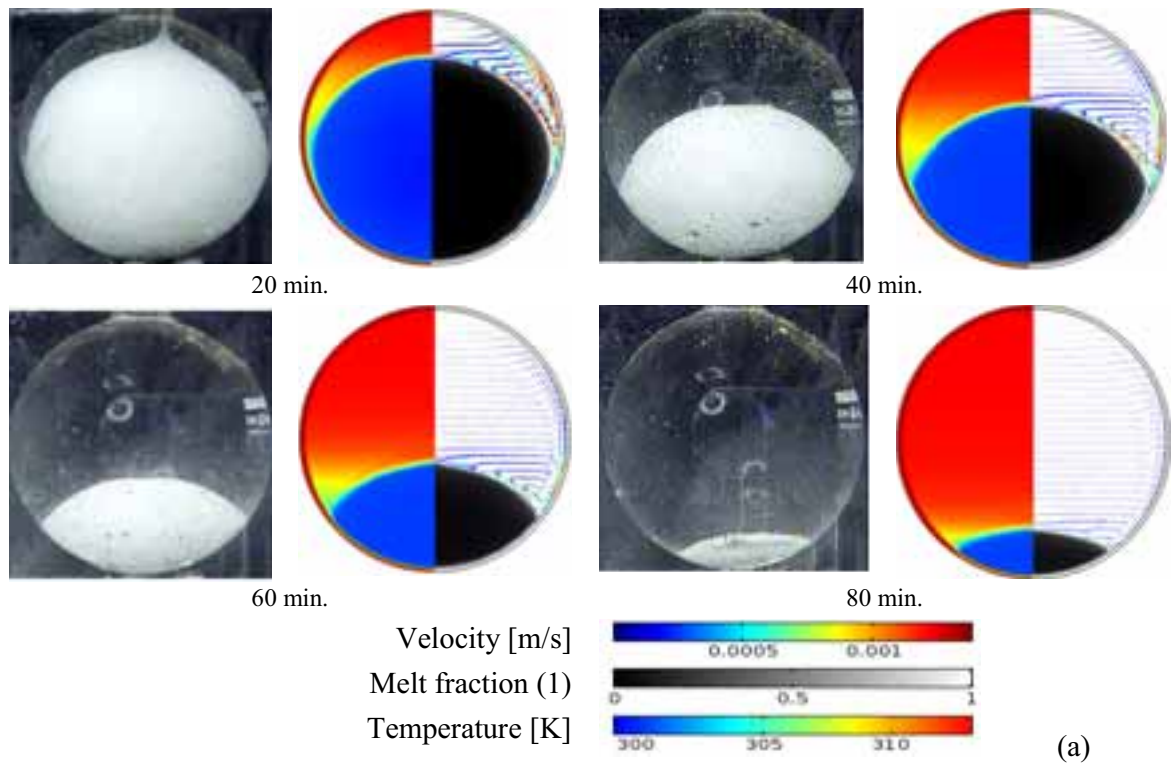


Fig. 2: Experimentally captured (Tan, 2008) and numerically predicted (a) melting front at various stages for $T_s = 40^\circ\text{C}$ (b) melt fraction as a function of time for $T_s = 45^\circ\text{C}$

In order to validate the model, simulations were performed for the experimental conditions reported by Tan

(2008). In their experiments, the n-octadecane was, used as PCM, filled in a 50.83 mm inner radius capsule and 1.5 mm wall thickness. Initially, the capsule was kept at 1°C less than the melting point (29°C), when $t > 0$ the outer surface of the capsule was fixed at 40°C. Simulation was performed for the same condition. The melting phase front, temperature and velocity distribution of the capsule during melting process are shown in Fig. 2(a) at 20 minutes intervals. Experimental photographs of melting process of the capsule are compared with the numerical results. In simulation results, the left side represents the temperature distribution and the right side represents the melt fraction and the velocity vector. Similarly, simulation was carried out for another case, where the outer surface temperature was fixed at 45°C. Fig. 2 (b) shows the comparison of experimentally measured (Tan, 2008) and numerically predicted melt fraction of the capsule. As can be seen in the figure, a good agreement is found between the numerical and experimental results.

Table 1. Thermo-physical properties of sodium nitrate

Properties	Sodium Nitrate
Density (kg/m ³)	
solid phase	2130
mushy zone	<i>Linear interpolation</i>
liquid phase	$\rho_{liq} = \rho_m / \beta(T - T_m) + 1$
ρ_m	1908
Dynamic viscosity (kg/m s)	$0.0119 - 1.53 \times 10^{-5} T$
Latent heat of fusion (J/kg)	178000
Melting temperature (°C)	306.8
Specific heat (J/kg/K)	$444.53 + 2.18 T$
Thermal expansion coef.(1/K)	6.6×10^{-4}
Thermal conductivity (W/m/K)	$0.3057 + 4.47 \times 10^{-4} T$

3. Results and discussion

Using the validated model, simulation was performed to predict the melting process of a nickel spherical shell (thickness=0.5 mm) of radius 10mm, completely filled with molten salt. Initially, the capsule was kept at 301.5 °C and at $t > 0$, the outer wall temperature was fixed at 311.5° C. Fig. 3 shows the temperature distribution and the corresponding melting process of the capsule at different stages. Each subfigure shows temperature distribution (left), melt fraction (right; black and white gradient), and natural convection flow velocity in the PCM liquid phase (right). During the initial stage of melting, the heat is transferred to the PCM through shell by conduction.

Once the melting process started at the inner surface of the shell, the natural convection starts to influences the melting process, the formed liquid PCM is heated by the inner surface of the shell. As the density changes between the solid and liquid phases, the solid part comes down due to gravity and the liquid flows upward and generates buoyancy driven flow. The heated fluid at the inner surface of the shell transfers the heat to the cold fluid close to the solid-fluid interface. Thus, an unsteady counter-clockwise circulating flow is formed above the solid part of the PCM during melting process. As a result, the melting process is faster at the top part of the solid phase and changes the spherical shape of the solid part into oblate spheroid shape as shown in the figure.

Influence of Stefan number and the capsule size on the melting process of the capsule is studied by various cases as shown in Table 2. By keeping the capsule size constant, simulations were carried out for cases 1-3 to study the effect of thermo-physical condition of the capsule (difference between the initial and outer wall temperature). Fig. 4 shows the melt fraction of the capsule as a function of time. As can be seen in the figure, an increase of temperature difference between the initial and outer wall temperature ($T_s - T_0$) can decrease the complete melting time. The complete melting time decreases about 8.5% and 4.5% respectively when increasing the temperature difference around 33% and 25%. The effect of pellet size on the melting rate for constant boundary conditions is presented in Fig. 5. The initial temperature and the wall temperature are

fixed and simulations were carried out for various capsule radii: 10, 15 and 20 mm. As expected, the complete melting time is decreased when the capsule size is reduced.

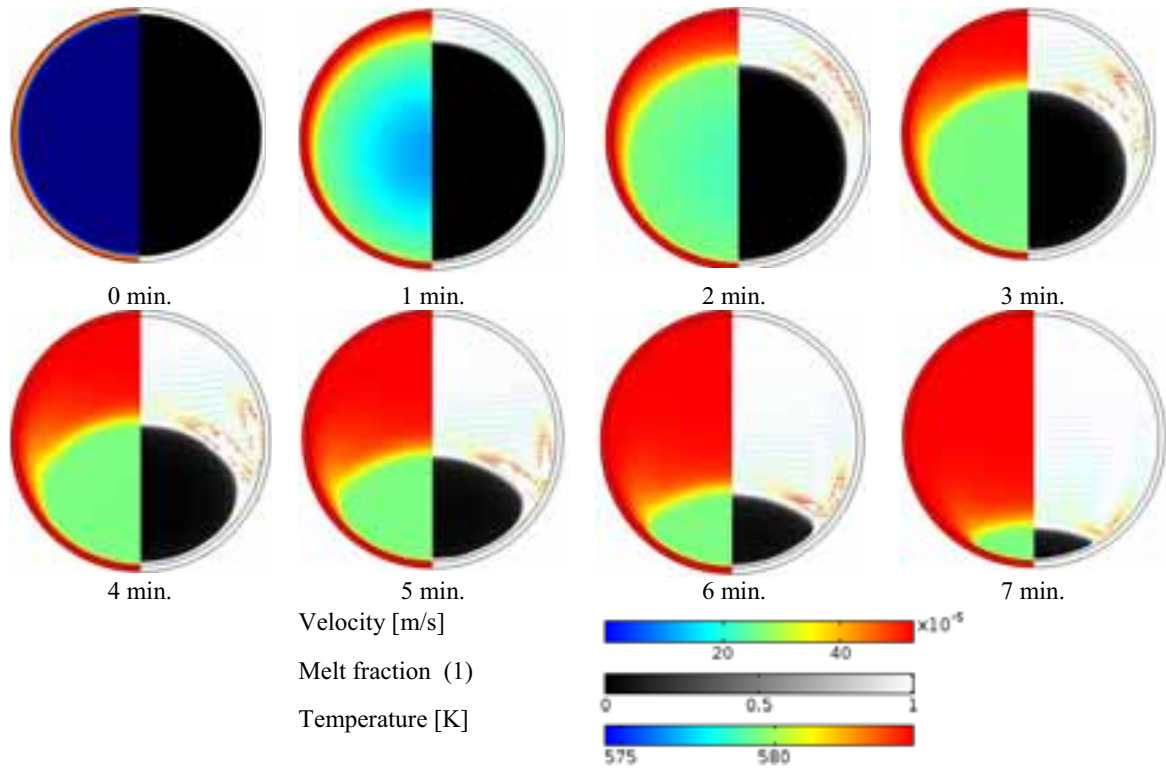


Fig. 3: Temperature distribution and the corresponding melting process of the capsule at different stages

Table 2 Analyzed cases

Case	Pellet radius (R_i) [m]	Initial Temperature (T_0) [°C]	Surface Temperature (T_s) [°C]	$T_s - T_0$ [°C]
1	0.010	301.5	311.5	10
2	0.010	299.0	314.0	15
3	0.010	296.5	316.5	20
4	0.015	299.0	314.0	15
5	0.020	299.0	314.0	15

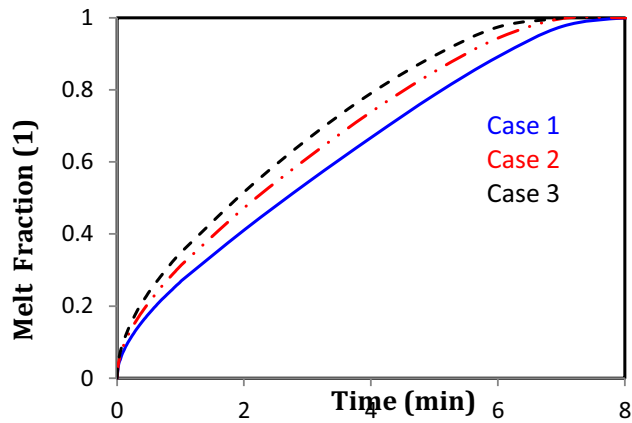


Fig.4: Melt fraction of the capsule as a function of time for various cases

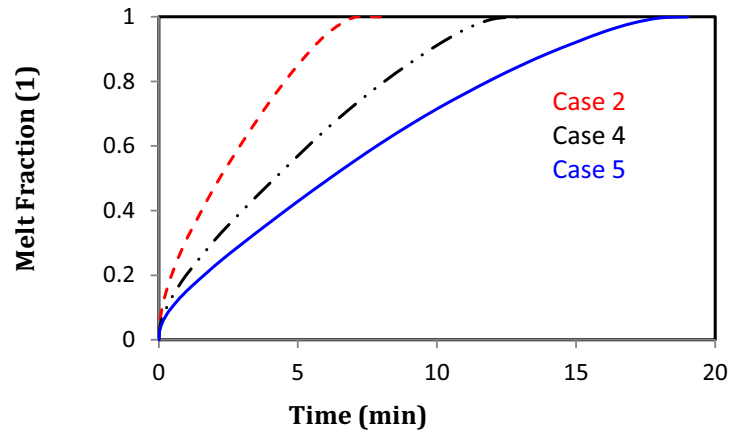


Fig. 5: Effect of pellet size on the melt fraction as a function of time.

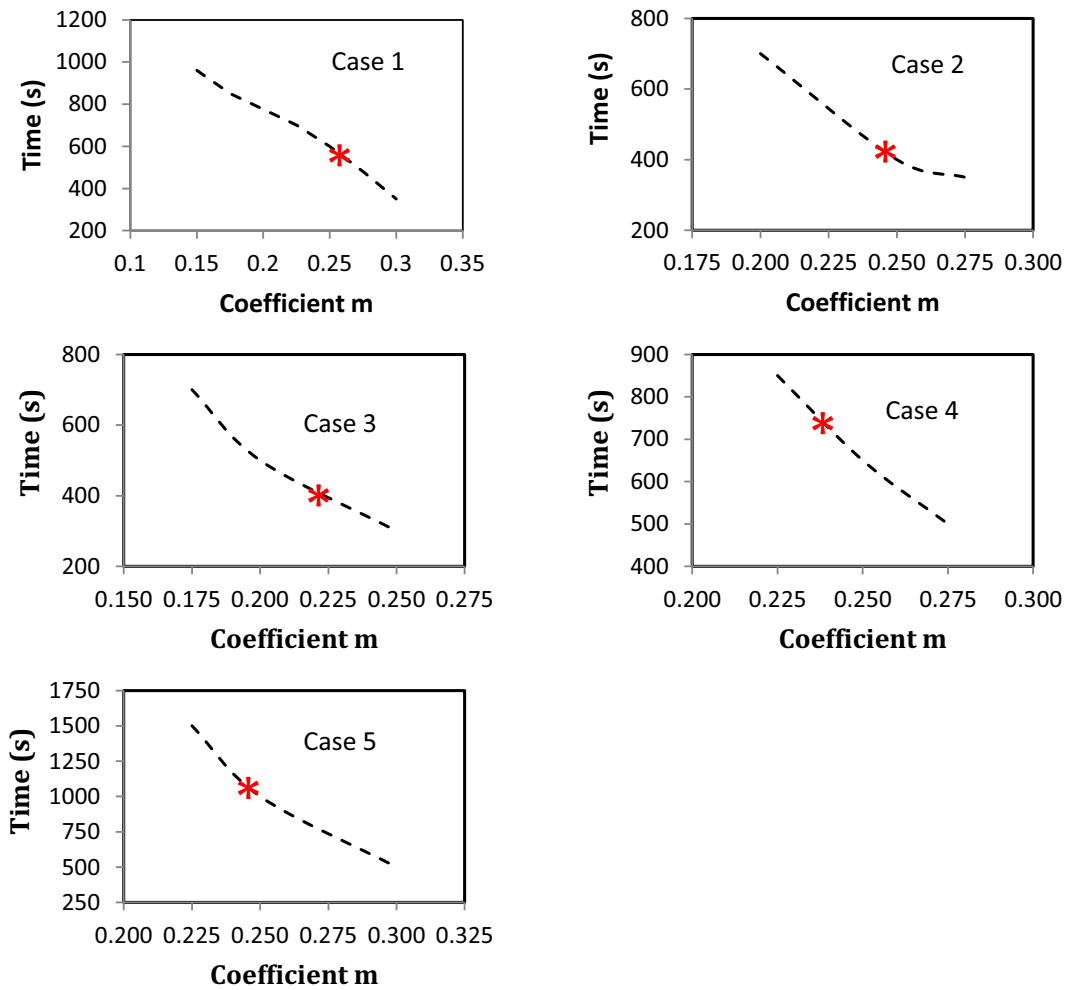


Fig. 6: Complete melting time as a function of coefficient m .

In order to study the performance of the thermal energy storage system packed with spherical PCM capsules, various packed bed numerical models have been developed in the past few decades (e.g. Bellan et al., 2014a, 2015a, 2015b). As explained in the previous sections, natural convection plays vital role during melting process. However, most of the melting process models only considered the thermal conduction due to complexity in incorporating the natural convection effect during melting process. The convective effect present in the liquid region during melting can be incorporated to the packed bed system by using the effective thermal conductivity correlation. To derive that correlation for the given set of cases as shown in Table 2, one dimensional conduction model for phase change process inside a capsule has been developed by enthalpy formulation method, based on the literature models (Bellan et al., 2014b; 2014c). The correlation given in eq. (7) is used to calculate the effective thermal conductivity

$$k_{ef} = k_L CRa^m \quad (\text{eq. 7})$$

In order to obtain the C and m coefficients, various values were assumed and the corresponding melt fraction evolution was predicted as a function of time. Then, the appropriate coefficients were obtained by comparing the 2D axi-symmetric model results obtained in the previous section. Initially, the coefficient of C was fixed at 0.18 (Bellan et al., 2015b), and calculations were made for case 1. Fig. 6 (case 1) shows the complete melting time predicted by the given correlation (Eq. 7) for various m coefficients. The complete melting time predicted by the 2D model is marked by asterisk symbol. Thus, the coefficient m is predicted for case 1, which is 0.26. Similarly, the coefficient m is predicted for other cases as shown in the figure. From this approximation, the generalized correlation is derived and given in eq. 8, which produces the same results of axisymmetric model.

$$k_{ef} = k_L 0.18Ra^{0.243} \quad (\text{eq. 8})$$

4. Conclusion

An axisymmetric model has been developed to predict the heat transfer, fluid flow due to natural convection, and phase change process. The developed model has been validated with reported experimental and numerical results. Then the influence of pellet size and the Stefan number on the heat transfer characteristics and the melting process have been studied. From the axisymmetric model results, an effective thermal conductivity correlation has been derived using one dimensional model. The derived correlation can be used to simulate the charging behavior of packed bed thermal energy storage system with spherical capsules.

Acknowledgment

Authors gratefully acknowledge the Spanish Ministry of Economy and Innovation through Plan Nacional I+D+i project no. ENE2011-29293; ‘‘Comunidad de Madrid’’ and ‘‘European Social Fund’’ for its financial support to the ALCCONES Project through the Programme of Activities between Research Groups (S2013/MAE-2985). The research leading to these results has received funding from the European Union Seventh Framework Programme (FP7/2007-2013) under grant agreement no. 60983.

5. References

- Archibold, A. R., Rahman, M.M., Goswami, D. Y., Stefanakos, E.K., 2014. Analysis of heat transfer and fluid flow during melting inside a spherical container for thermal energy storage, *Applied Thermal Engineering* 64, 396-407.
- Assis, E., Katsman, L., Ziskind, G., Letan R., 2007. Numerical and experimental study of melting in a spherical shell. *International Journal of Heat and Mass Transfer* 50, 1790–1804.
- Bareiss, M., Beer, H., 1984. An analytical solution of the heat transfer process during melting of an unfixed solid phase change material inside a horizontal tube, *Int. J. Heat Mass Transfer* 27, 739-746.
- Bellan, S., González-Aguilar, J., Romero, M., Rahman, M.M., Goswami, D. Y., Stefanakos, E.K., 2014a. Numerical Modeling of Thermal Energy Storage System, ASME 2014 8th International Conference on

Energy Sustainability collocated with the ASME 2014 12th International Conference on Fuel Cell Science, Engineering and Technology, doi:10.1115/ES2014-6382.

Bellan, S., González-Aguilar, Archibold, A. R., J., Romero, M., Rahman, M.M., Goswami, D. Y., Stefanakos, E.K., 2014b. Transient numerical analysis of storage tanks based on encapsulated PCMs for heat storage in concentrating solar power plants, *Energy Procedia* 57, 672-681.

Bellan, S., González-Aguilar, J., Romero, M., Rahman, M.M., Goswami, D. Y., Stefanakos, E.K., David, C., 2014c. Numerical analysis of charging and discharging performance of a thermal energy storage system with encapsulated phase change material, *Applied Thermal Engineering* 71,481-500.

Bellan, S., Tanvir E. A., González-Aguilar, J., Romero, M., Rahman, M.M., Goswami, D. Y., Stefanakos, E.K., 2015a. Numerical and experimental studies on heat transfer characteristics of thermal energy storage system packed with molten salt PCM capsules, *Applied Thermal Engineering* 90, 970-979.

Bellan, S., González-Aguilar, J., Romero, M., Rahman, M.M., Goswami, D. Y., Stefanakos, E.K., 2015b. Numerical Investigation of PCM-based Thermal Energy Storage System, *Energy Procedia*, 69, 758-768

COMSOL Multiphysics Version 4.3, COMSOL AB, Stockholm, Sweden, 2013

Felix, R.A., Solanki, S.C., Saini, J.S., 2006. Experimental and numerical analysis of melting of PCM inside a spherical capsule, in: 9th AIAA/ASME Joint Thermophysics and Heat Transfer Conf. Proc., AIAA- 2006-3618.

Hosseinizadeh, S.F., Rabienataj Darzi, A.A., Tan F.L., J.M. Khodadadi., 2012. Unconstrained melting inside a sphere. 63, 55-64. *Int. J. Therm. Sci.* 63, 55-64.

Ismail, K.A.R., Henríquez, J.R., 2000. Solidification of pcm inside a spherical capsule. *Energy Conversion and Management*. 41, 173-187.

Moore, F.E., Bayazitoglu, Y., 1982. Melting within a spherical enclosure, *J. Heat Transfer* 104, 19-23.

Roy, S.K., Sengupta, S.,1987. The melting process within spherical enclosures, *J. Heat Transfer* 109 460-462.

Tan, F.L., 2008. Constrained and unconstrained melting inside a sphere. *International Communications in Heat and Mass Transfer*. 35, 466–475.

Tanvir E. A., Jaspreet,D., Goswami, D. Y., Stefanakos, E.K., 2015. Macroencapsulation and characterization of phase change materials for latent heat thermal energy storage systems, *Applied Energy*, 154, 92-101.